

# Characterization of Cancer Stem Cells in Renal Clear Cell Carcinoma

Reuben Cane<sup>1</sup>, Andrew Kennedy-Smith<sup>1,2</sup>, Helen D Brasch<sup>1</sup>, Stephanie Savage<sup>1</sup>, Reginald W Marsh<sup>1,3</sup>, Tinte Itinteang<sup>1</sup>, Swee T Tan<sup>1,4\*</sup>

<sup>1</sup>Gillies McIndoe Research Institute, Wellington, New Zealand

<sup>2</sup>Department of Urology, Wellington Regional Hospital, Wellington, New Zealand

<sup>3</sup>University of Auckland, Auckland, New Zealand

<sup>4</sup>Wellington Regional Plastic, Maxillofacial & Burns Unit, Hutt Hospital, Wellington, New Zealand

\*Corresponding author: Swee T Tan, ONZM, MBBS PhD FRACS, Gillies Mc Indoe Research Institute, PO Box 7184, Newtown 6242, Wellington, New Zealand, Tel: +64 4 2820366; Email: [swee.tan@gmri.org.nz](mailto:swee.tan@gmri.org.nz)

## Abstract

There is increasing literature showing the presence of cancer stem cells (CSCs) in renal clear cell carcinoma (RCCC) which is associated with poor prognosis. Characterization of CSCs may lead to better understanding and treatment of RCCC.

4µm-thick formalin-fixed paraffin-embedded RCCC samples from ten patients underwent 3,3-diaminobenzidine (DAB) immunohistochemical (IHC) staining for the embryonic stem cell (ESC) markers NANOG, SOX2, OCT4, c-MYC, KLF4 and progenitor cell marker CD44. NanoString (n = 4) and *in-situ* hybridization (ISH, n = 6) mRNA analyses were performed on RCCC samples to investigate transcript expression of these ESC markers. Cell counting was performed on the IHC- and ISH-stained slides and statistical analyses were performed using t-tests. Immunofluorescence (IF) IHC staining was performed on two RCCC samples to localize the expression of these ESC markers.

DAB IHC staining demonstrated expression of NANOG, SOX2, OCT4, c-MYC, KLF4 and CD44 in all ten RCCC samples. Cell counting revealed a high abundance of SOX2, NANOG and c-MYC and a low abundance of KLF4 and OCT4. ISH and NanoString analyses confirmed the presence of mRNA transcripts for NANOG, OCT4, c-MYC and KLF4 while SOX2 was detected only by ISH. IF IHC staining showed expression of OCT4 in cells expressing SOX2, NANOG and KLF4. c-MYC was expressed by cells expressing SOX2 and NANOG, with a subset also expressing KLF4. These findings suggest the presence of CSC subpopulations within RCCC with a lower proportion of CSCs expressing the more primitive markers OCT4 and KLF4, and a higher proportion expressing the more downstream markers SOX2, NANOG and c-MYC.

**Keywords:** cancer stem cells; embryonic stem cells; expression; renal cell carcinoma; renal clear cell carcinoma.

Received date: April 1, 2019

Accepted date: May 2, 2019

Published date: May 7, 2019

**Citation:** Cane, R., et al. Characterization of Cancer Stem Cells in Renal Clear Cell Carcinoma (2019) J Stem Cell Regen Biol 5(1): 6-17.

**Copy Rights:** © 2019 Swee, T. T. This is an Open access article distributed under the terms of Creative Commons Attribution 4.0 International License.

## Introduction

Renal cell carcinoma (RCC) is the ninth most common cancer, with approximately 338,000 new cases annually, resulting in 144,000 deaths worldwide in 2012<sup>[1]</sup>. The incidence of RCC is highest in developed countries attributed to the common use of imaging<sup>[1]</sup>.

Established risk factors for RCC include obesity, hypertension and smoking<sup>[2]</sup>, and protective factors include physical activity and legume consumption<sup>[2,3]</sup>. Renal clear cell carcinoma (RCCC) constitutes 80-85% of all RCCs, contributing significantly to the morbidity and mortality from RCC<sup>[1]</sup>.

Current treatment for localized RCC is partial or total nephrectomy which is associated with a 40% local recurrence rate<sup>[4]</sup> with 30% of patients eventually developing metastatic disease, which typically resists chemotherapy and radiotherapy<sup>[5]</sup>. Advanced disease is treated with combined therapies including total nephrectomy and systemic targeted-drug therapies. Targeted therapies include mammalian target of rapamycin inhibitors that reduce both cellular growth and proliferation<sup>[6-8]</sup> and vascular endothelial growth factor receptor (VEGFR) inhibitors that reduce the angiogenic ability of the tumor, along with vascular endothelial growth factor (VEGF) ligand-directed therapy, which can bind and neutralize circulating VEGF to decrease tumor growth<sup>[6,7]</sup>. However, despite the use of targeted therapies for advanced disease, the prognosis of RCC remains dismal with a 10% 5-year survival rate for patients with metastatic disease<sup>[5-8]</sup>. Immunotherapy agent nivolumab has demonstrated superior efficacy over everolimus for patient with metastatic RCC that failed previous line of tyrosine kinase inhibitor<sup>[9]</sup>. The combination of nivolumab/ipilimumab also demonstrated superior efficacy over sunitinib as first-line therapeutic agents<sup>[10]</sup>.

Genetic links to the development of RCC include mutations to the Von Hippel Lindau (VHL) gene and deletions of the short arm of chromosome 3<sup>[11]</sup>. Loss of VHL protein has been attributed to the inability to degrade hypoxia induced factor resulting in changes to cells that contribute to the development of RCC<sup>[11]</sup>.

It has been proposed that tumor development and proliferation is driven by cancer stem cells (CSCs) that possess self-renewal and pluripotent properties and are responsible for metastasis and recurrence<sup>[8-12]</sup>. Research has shown that many types of cancer express embryonic stem cell (ESC) markers allowing the identification of CSCs using the ESC markers NANOG, OCT4, SOX2, KLF4, c-MYC and progenitor cell marker CD44<sup>[13-15]</sup>. The importance of these proteins in maintaining pluripotency and self-renewal capabilities of ESC like cells<sup>[16,17]</sup> was highlighted by Takahashi and Yamanaka<sup>[16]</sup> who successfully transformed adult human fibroblasts to ESC-like cells by inserting the OCT4, SOX2, c-MYC and KLF4 genes, while Thompson<sup>[17]</sup> showed similar results by substituting c-MYC and KLF4 with LIN28 and NANOG.

NANOG, OCT4 and SOX2 are transcription factors that play a central role in maintaining pluripotency of ESCs and their ability for self-renewal<sup>[13-18]</sup>. OCT4 is a transcription factor that is key for the self-renewal and pluripotent abilities of ESCs<sup>[14-18]</sup>. KLF4 is a protein critical for the regulation of cellular proliferation, differentiation and self-renewal<sup>[19-21]</sup>. SOX2 is another transcription factor required to maintain the proliferative ability and pluripotency of ESCs<sup>[14-18]</sup>. c-MYC which is important for promoting cell proliferation and differentiation, has been found to be present at elevated levels in RCC<sup>[18-22]</sup>. CD44, a progenitor cell marker involved in cell adhesion and migration, are associated with increased cancer aggressiveness, metastatic disease and morbidity of RCC<sup>[15,23,24]</sup>.

Earlier literature on RCC have used progenitor cell markers CD44 and CD133 as markers of CSCs in RCC<sup>[25,26]</sup> and more recent literature suggests the presence of CSCs in RCC that express ESC markers such as OCT4, NANOG, SOX2, KLF4 and c-MYC<sup>[5,12,14]</sup>. Expression of CSC markers in RCC has been shown to be associated with a poorer prognosis<sup>[15,21,27]</sup>. Interestingly, KLF4 is expressed at lower levels in cancer compared to normal tissues suggesting it acts as a tumor suppressor gene<sup>[21]</sup>. Liu et al.,<sup>[27]</sup> report up-regulation of c-MYC in RCC, suggesting its role as an oncogene. CD44 has previously been found to be expressed in RCC and has been linked to poorer prognosis and treatment resistance<sup>[15,23]</sup>.

Current cancer treatments do not target CSCs, highlighting the need for the identification and characterization of CSCs, potentially leading to the development of novel therapy by targeting this population within this tumor<sup>[8]</sup>.

In this study we identified and characterized CSCs in RCCC using IHC staining, *in situ* hybridization (ISH) and NanoString mRNA analyses using CD44 as a marker for CSCs as in previous publications and ESC markers OCT4, NANOG, SOX2, KLF4 and c-MYC.

## Materials and Methods

### Tissue Samples

RCCC tissue samples from six female and four male patients, aged 65-77 (mean 69.7) years were sourced from the Gillies McIndoe Research Institute Tissue Bank and used in this study, which was approved by the Northern B Health and Disability Ethics Committee (Ref. 16/NTB/10). Informed written consent was obtained from all participants.

### Histochemical Staining and Immunochemical Staining

Hematoxylin and eosin (H&E) staining was performed on 4µm thick formalin-fixed paraffin-embedded sections of RCCC to confirm the presence of RCCC on the slides, by an anatomical pathologist (HDB). All sections underwent 3,3-diaminobenzidine (DAB) IHC staining carried out on the Leica Bond Rx auto-stainer (Leica, Nussloch, Germany) as previously described<sup>[28]</sup>. Primary antibodies used for IHC staining were CD44 (1:1500; cat #MRQ-13; Cell Marque, Rocklin, CA, USA), NANOG (1:100; cat#ab80892,

Abcam, Cambridge, MA, USA), OCT4 (1:30; cat#MRQ-10, Cell Marque), SOX2 (1:200; cat#PA1-094, Thermo Fisher Scientific, Rockford, IL, USA), KLF4 (1:200; cat#NBP2-24749SS, Novus Biologicals LLC, Littleton, CO, USA) and c-MYC (1:1000; cat#9E10, Abcam).

To demonstrate co-expression of the proteins, two representative RCCC samples from the original cohort of ten patients underwent immunofluorescence (IF) IHC staining using the same primary antibodies as well as using a combination of Vectafluor Excel anti-rabbit 594 (ready-to-use; cat# VEDK -1594, Vector Laboratories, Burlingame, CA, USA) and Alexa Fluor anti-mouse 488 (1:500; cat# A21202, Life Technologies) to detect combinations of NANOG, OCT4, SOX2, c-MYC and KLF4.

Human tissues used for positive controls for the primary antibodies were seminoma for NANOG and OCT4<sup>[29]</sup>, skin for SOX2<sup>[30]</sup>, breast cancer for KLF4<sup>[19]</sup>, prostate tissue for c-MYC<sup>[31]</sup> and tonsil for CD44<sup>[32]</sup>. Negative controls were performed using a section of RCCC tissue with the use of primary isotype mouse (ready-to-use; cat# IR750, Dako, Copenhagen, Denmark) and rabbit (ready-to-use; cat# IR600, Dako) anti-bodies, to determine the specificity of the amplification cascade.

### Cell Counting and Statistical Analyses

Counting of cells that stained positively on DAB IHC staining for the ESC markers NANOG, SOX2, OCT4, c-MYC and KLF4 was carried out on six fields of view, containing the highest number of positive staining for each marker and for each RCCC sample at 400x magnification. A combined total was taken and the proportion of cells that stained positively for each CSC marker was then calculated, as previously described<sup>[33]</sup>.

Statistical analysis with related sample t-tests was performed using SPSS Statistics version 22.  $\chi^2$  tests were also carried out to investigate the presence of significant difference in the proportions of cells staining positively between the markers.

### In-situ Hybridization

Representative 4 $\mu$ m-thick formalin-fixed paraffin-embedded sections of six RCCC samples from the original cohort of ten patients used for the DAB IHC staining underwent ISH staining, carried out on the Leica Bond Rx auto-stainer and detected using the ViewRNA™ eZ Detection Kit 1-Plex (Affymetrix, Santa Clara, CA, USA), as previously described<sup>[28]</sup>. The probes used were as follows: NANOG (NM\_024865), SOX2 (NM\_003106), OCT4 (NM\_002701), c-MYC (NM\_002467), KLF4 (NM\_004235), all sourced from Affymetrix. Human positive controls used were seminoma for NANOG and OCT4, skin for SOX2, prostate tissue for c-MYC and breast cancer for KLF4. A negative control was performed on each run using the *Baccillus* (L38424) probe.

### Image Analysis

DAB IHC- and ISH-stained slides were viewed and the images were taken using the Olympus BX53 light microscope fitted with an Olympus DP21 digital camera. They were processed with the cellSens 2.0 Software (Olympus, Tokyo, Japan). IF IHC-stained slides were viewed and the images were taken using the Olympus FV1200 biological confocal laser-scanning microscope and processed using the 2D deconvolutional module of cell Sens Dimension 1.11 software (Olympus).

### NanoString mRNA Analysis

RNA was extracted from four snap-frozen RCCC samples of the original cohort of ten patients used for the DAB IHC staining, and analyzed using the NanoStringnCounter™ Gene Expression Assay (NanoString Technologies, Seattle, WA, USA), as previously described<sup>[18,24]</sup>. RNA was extracted from tissues using a RN easy Mini Kit (Qiagen, Hilden, Germany) and quantitated by Qubit® 2.0 Fluorometer (Life Technologies). The RNA was quantitated using a Qubit® 2.0 fluorometer (Life Technologies) and then subjected to 2100 Bioanalyzer (Agilent Technologies, Santa Clara, CA, USA) for integrity analysis prior to NanoStringnCounter™ expression analysis assay, which was completed by New Zealand Genomics Ltd (Dunedin, NZ). Probes for the mRNA genes encoding NANOG (NM\_024865.2), SOX2 (NM\_003106.2), OCT4 (NM\_002701.4), c-MYC (NM\_002467.3), KLF4 (NM\_004235.4) and the house-keeping gene GUSB (NM\_000181.1) were designed and manufactured by NanoString Technologies.

## Results

### Histochemical and DAB Immunohistochemical Staining

H&E staining confirmed the presence of RCCC on the slides (Fig. 1A) for all ten RCCC samples used for DAB IHC staining, which demonstrated cytoplasmic staining for CD44 (Fig. 1B), moderate to strong nuclear staining for NANOG (Fig. 1C) and SOX2 (Fig. 1D) weak nuclear staining for OCT4 (Fig. 1E), moderate to strong nuclear staining for c-MYC (Fig. 1F) and moderate cytoplasmic staining for KLF4 (Fig. 1G). There was no staining for these ESC markers on a normal kidney sample (data not shown).

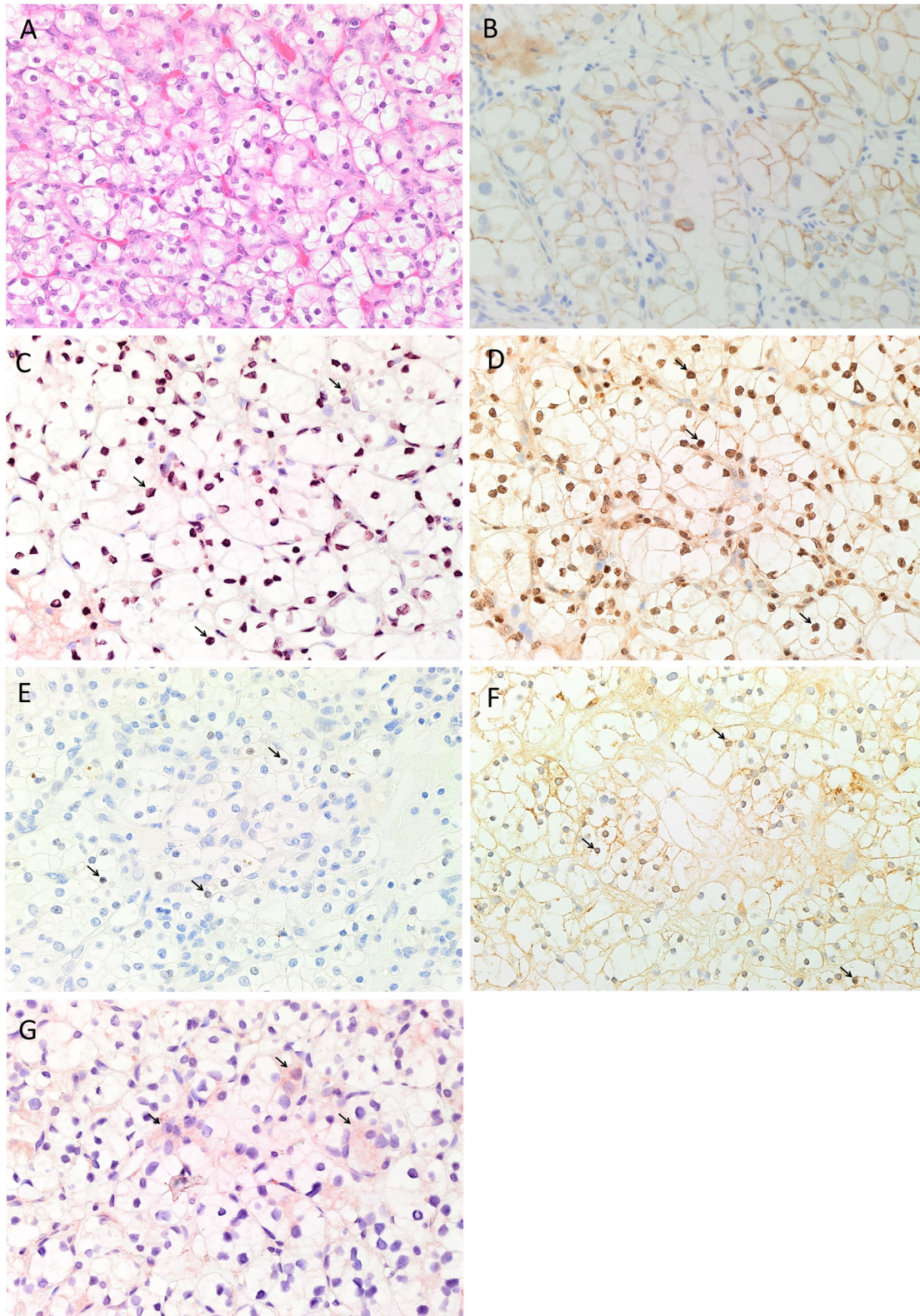


**Figure 1:** Representative hematoxylin and eosin stained section of renal clear cell carcinoma (A) and 3,3-diaminobenzidine immunohistochemical stained sections (B-G) showing membranous staining for CD44 (B, purple), nuclear staining of NANOG (C, purple, *arrows*), SOX2 (D, brown, *arrows*), OCT4 (E, brown, *arrow*) and c-MYC (F, purple, *arrows*) and cytoplasmic staining of KLF4 (G, purple, *arrows*). Nuclei were counter-stained with hematoxylin (A-G, blue). Original magnification: 400x.

**Positive control human tissues:** seminoma for NANOG (Fig. 2A), skin for SOX2 (Fig. 2B), seminoma for OCT4 (Fig. 2C), prostate tissue for c-MYC (Fig. 2D), breast cancer for KLF4 (Fig. 2E) and tonsil for CD44 (Fig. 2F) showed the expected staining pattern for each marker. As expected there was minimal staining of RCCC tissue in both the DAB IHC mouse and rabbit isotype negative controls (Fig. 2G).

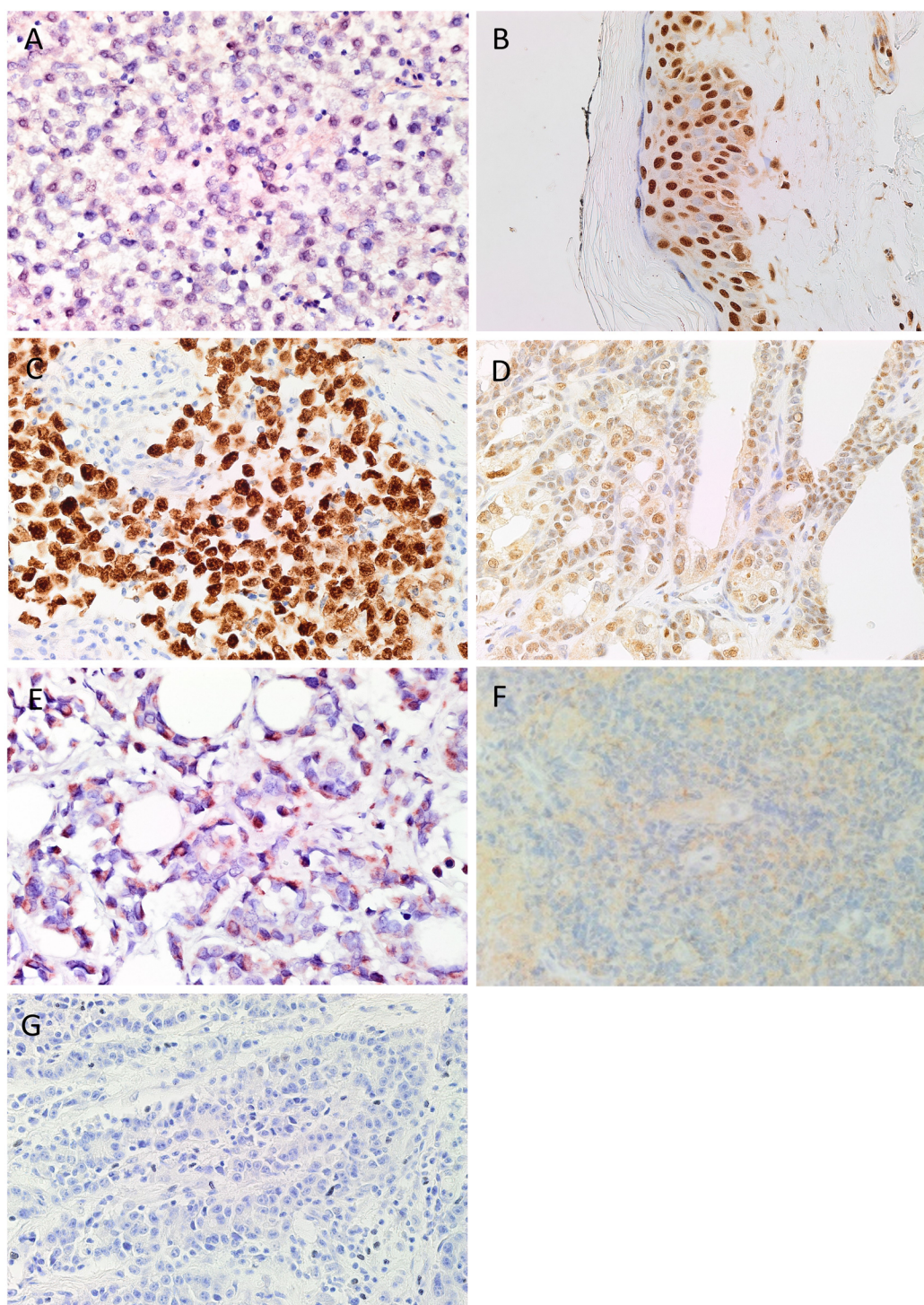


**Figure 2:** Positive human control tissues of 3,3-diaminobenzidine immunohistochemical (DAB IHC)-stained sections of seminoma for NANOG (A, purple), skin for SOX2 (B, brown), seminoma for OCT4 (C, brown), prostate tissue for c-MYC (D, brown), breast cancer for KLF4 (E, purple) and tonsil for CD44 (F, brown). Negative control (G) performed on a renal clear cell carcinoma section using isotype negative controls for the DAB IHC, confirmed specificity of the primary isotype antibody (G). Nuclei were counter-stained with hematoxylin (A-G, blue). Original magnification: 400x.

### Cell Counting and Statistical Analyses

Cell counting of the DAB IHC-stained slides demonstrated relatively high proportions of cells stained positively for SOX2 (83%), NANOG (86%), and c-MYC (80%); a lower proportion of cells stained positively for KLF4 (14%) and for OCT4 (8%) (Fig. 3). Statistical analysis demonstrated a significant difference between the proportion of cells that stained positively for OCT4 and KLF4 compared to the proportion of cells that stained positively for the other markers ( $p < 001$ ).

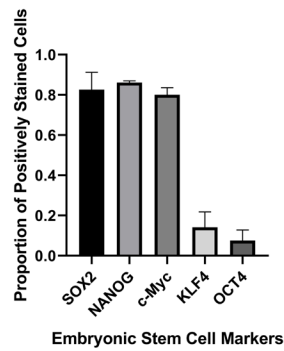


**Figure 3:** Proportion of cells stained positively for NANOG, SOX2, c-MYC, KLF4 and OCT4 on DAB IHC-stained slides of renal clear cell carcinoma samples from six patients. Statistical analysis showed these results to be significant ( $p < 0.001$ ). Error bars represent mean  $\pm$  standard deviation.

### Immunofluorescence Immunohistochemical Staining

To demonstrate co-expression of ESC markers, IF IHC staining was carried out on two representative RCCC samples from the original cohort of ten patients included for the DAB IHC staining. The expression of CD44 (Fig. 4A-C, green) was localized to the cell membrane of the cells that also expressed nuclear staining for SOX2 (Fig. 4A, red), NANOG (Fig. 4B, red) and KLF4 (Fig. 4C, red). OCT4 (Fig. 4D-F, green) was localized to the nuclei of a subpopulation of the cells that also expressed SOX2 (Fig. 4D, red), NANOG (Fig. 4E, red) and KLF4 (Fig. 4F which appeared orange white arrows). The expression of c-MYC (Fig. 4G-I, green, *white arrows*) was localized to the cytoplasm of the cells that also expressed SOX2 (Fig. 4G, red). NANOG (Fig. 4H, red), and intriguingly in a subpopulation that also expressed KLF4 (Fig. 4I, red, *white arrows*).

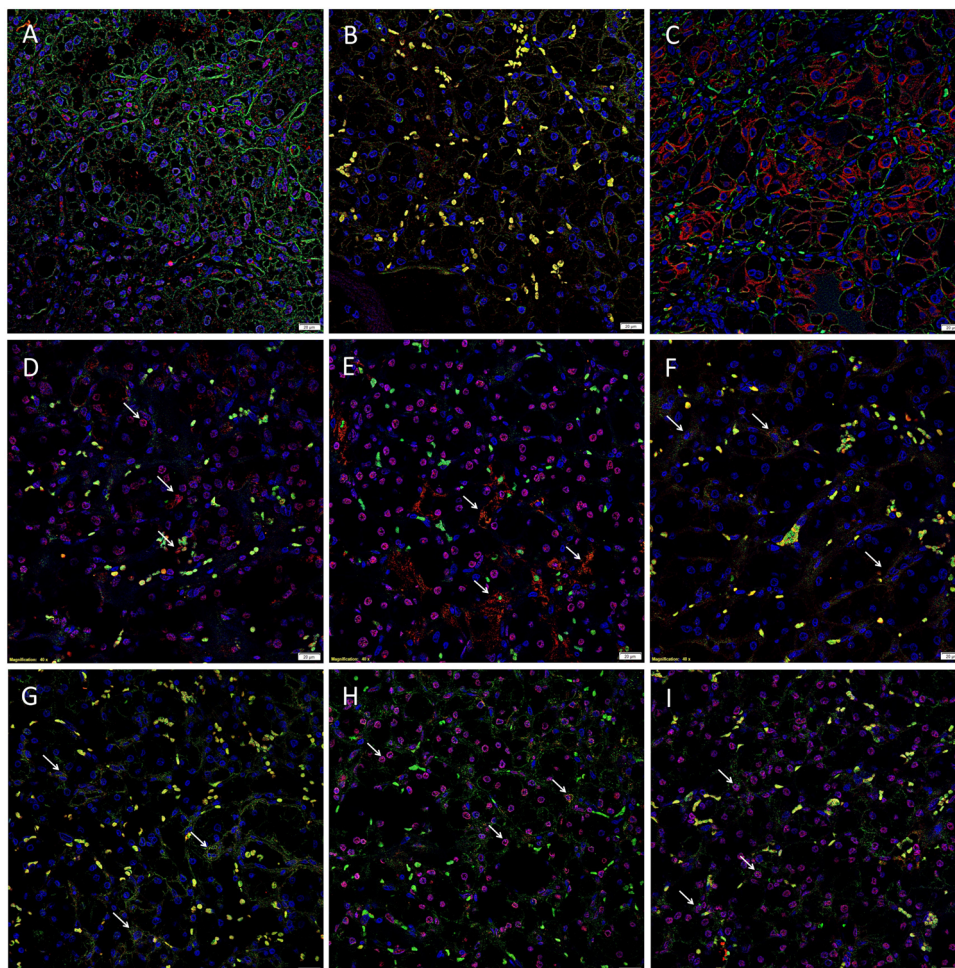


**Figure 4:** Representative immunofluorescence immunohistochemical stained sections of renal clear cell carcinoma demonstrating the co-expression of CD44 (A-C) with SOX2 (A), NANOG (B) and KLF4 (C). Staining for OCT4 (D-F, green) performed with SOX2 (D, red), NANOG (E, red) and KLF4 (F, red) c-MYC (G-I, green) was co-expressed with SOX2 (G, red) and NANOG (H, red) with only a proportion that also expressed KLF4 (I, red, *white arrows*). Cell nuclei are displayed by 4'6'-diamidino-2-phenylindole staining (A-I, blue). Scale bars: 20µm.

Images of the individual IF IHC stains shown in Figure 4 are presented in Figure 5. As expected, there was minimal staining of sections of RCCC in IF IHC staining mouse and rabbit isotype negative controls (Fig. 5S).

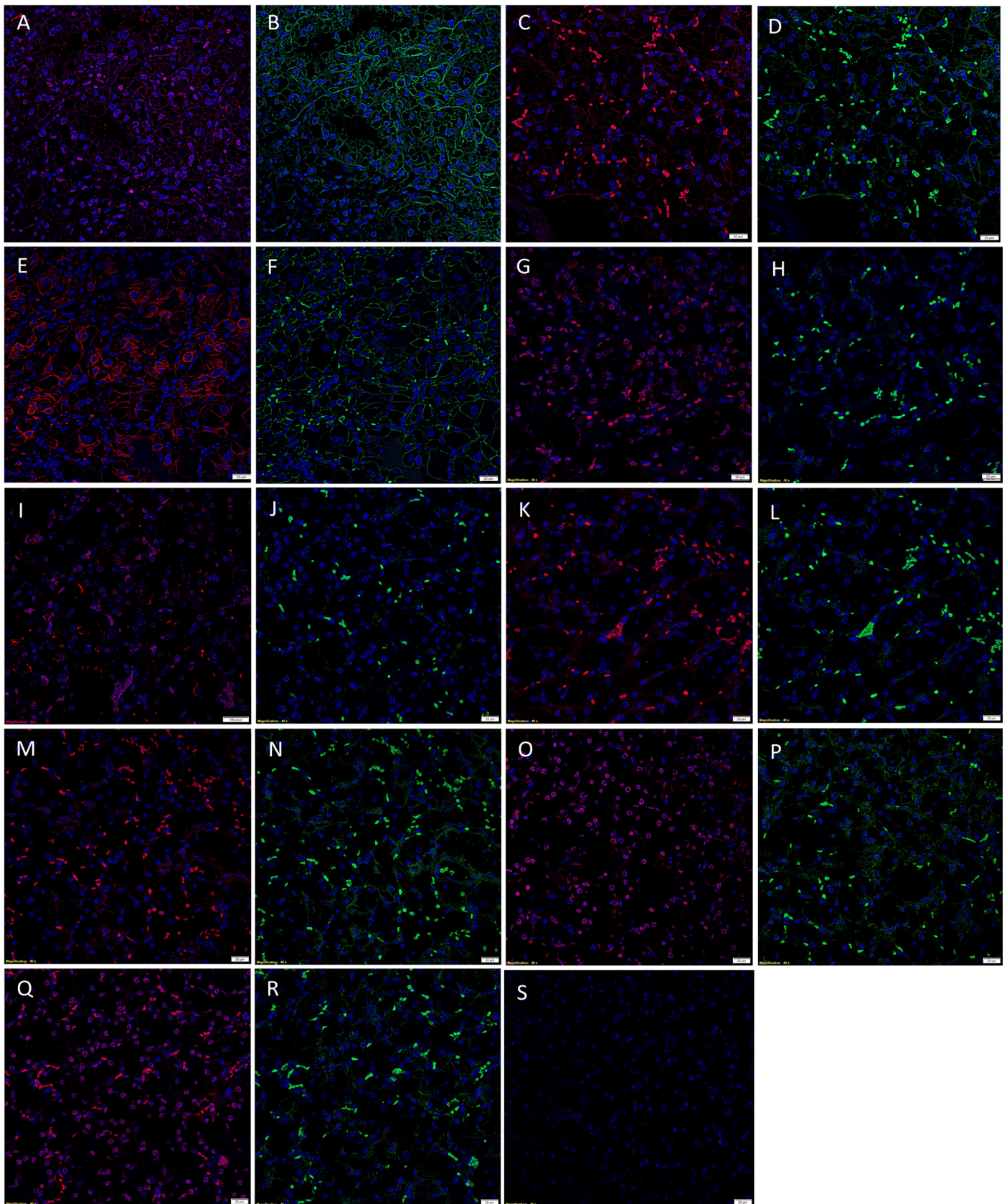


**Figure 5:** Split images of immunofluorescence immunohistochemical-stained sections of renal clear cell carcinoma shown in Figure 4 demonstrating expression of SOX2 (A, red) and CD44 (B, green), NANOG (C, red) and CD44 (D, green), KLF4 (E, green) and CD44 (F, green), SOX2 (G, red) and OCT4 (H, green), NANOG (I, red) and OCT4 (J, green), KLF4 (K, green) and OCT4 (L, green), KLF4 (M, green) and c-MYC (N, green), SOX2 (O, red) and c-MYC (P, green), NANOG (Q, red) and c-MYC (R, green). An isotype negative control section of RCCC showed specificity of the fluorescent antibody (S). Cell nuclei (A-S, blue) are displayed by 4'6'-diamidino-2-phenylindole staining. Scale bars: 20µm.

### NanoString mRNA Analysis

NanoString mRNA analysis confirmed the presence of mRNA transcripts for NANOG, OCT4, c-MYC and KLF4 while SOX2 was below detectable levels (Fig. 6). RNA integrity analysis confirmed that 2 of the 4 samples had RIN > 7.

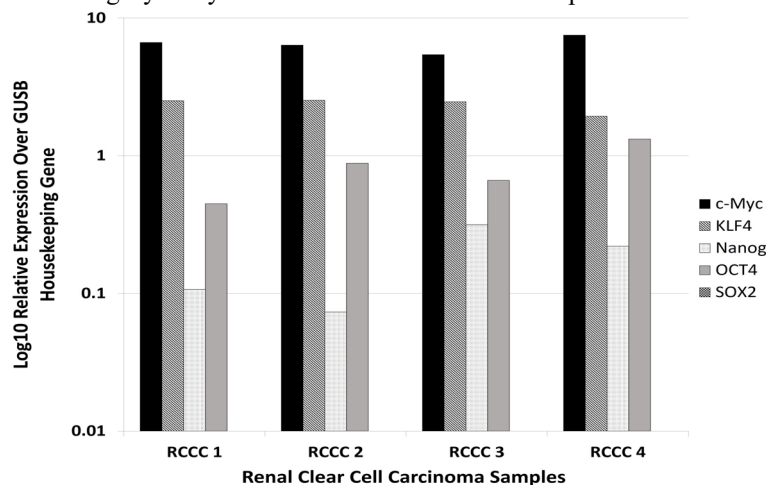


**Figure 6:** NanoString mRNA analysis showing relative expression of the embryonic stem cell marker genes over the housekeeping gene GUSB, confirming the presence of mRNA transcripts of NANOG, c-MYC, KLF4 and OCT4 in renal clear cell carcinoma, while SOX2 was below detectable levels.

### In-situ Hybridization

ISH confirmed the presence of mRNA transcripts for NANOG (Fig. 7A), SOX2 (Fig. 7B), OCT4 (Fig. 7C), c-MYC (Fig. 7D) and KLF4 (Fig. 7E) in all six RCCC samples examined.

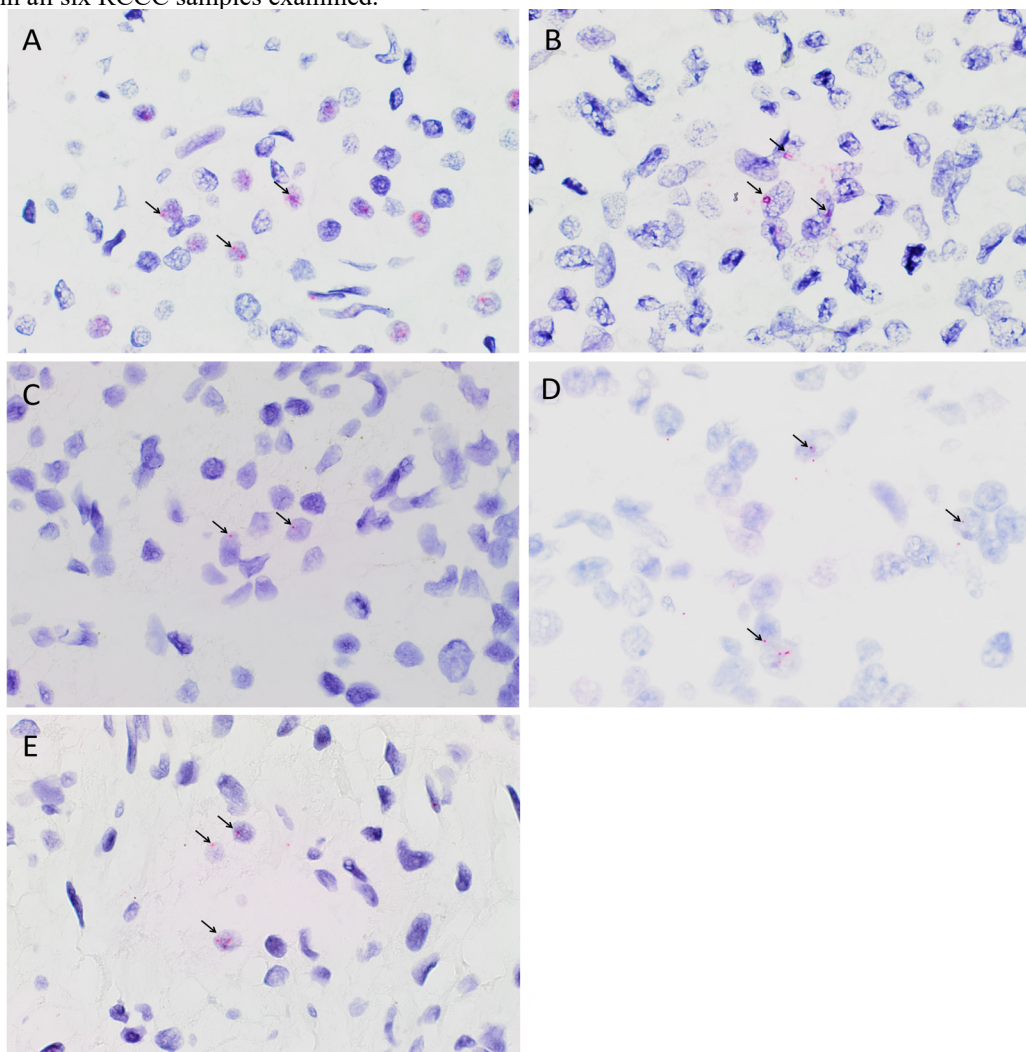


**Figure 7:** Representative *in situ* hybridization stained sections of renal clear cell carcinoma demonstrating mRNA expression of NANOG (A, pink, arrows), SOX2 (B, pink, arrows), OCT4 (C, pink, arrows), c-MYC (D, pink, arrows) and KLF4 (E, pink, arrows). Nuclei were counter-stained

with hematoxylin (A-E , blue). Original magnification: 1000x.

Appropriate staining was seen on positive control tissues for NANOG (Fig. 8A), SOX2 (Fig. 8B), OCT4 (Fig. 8C), c-MYC (Fig. 8D) and KLF4 (Fig.8E) indicating the presence of mRNA transcripts in the controls. The negative control performed on each run showed no mRNA transcripts for any of the markers (Fig. 8F).

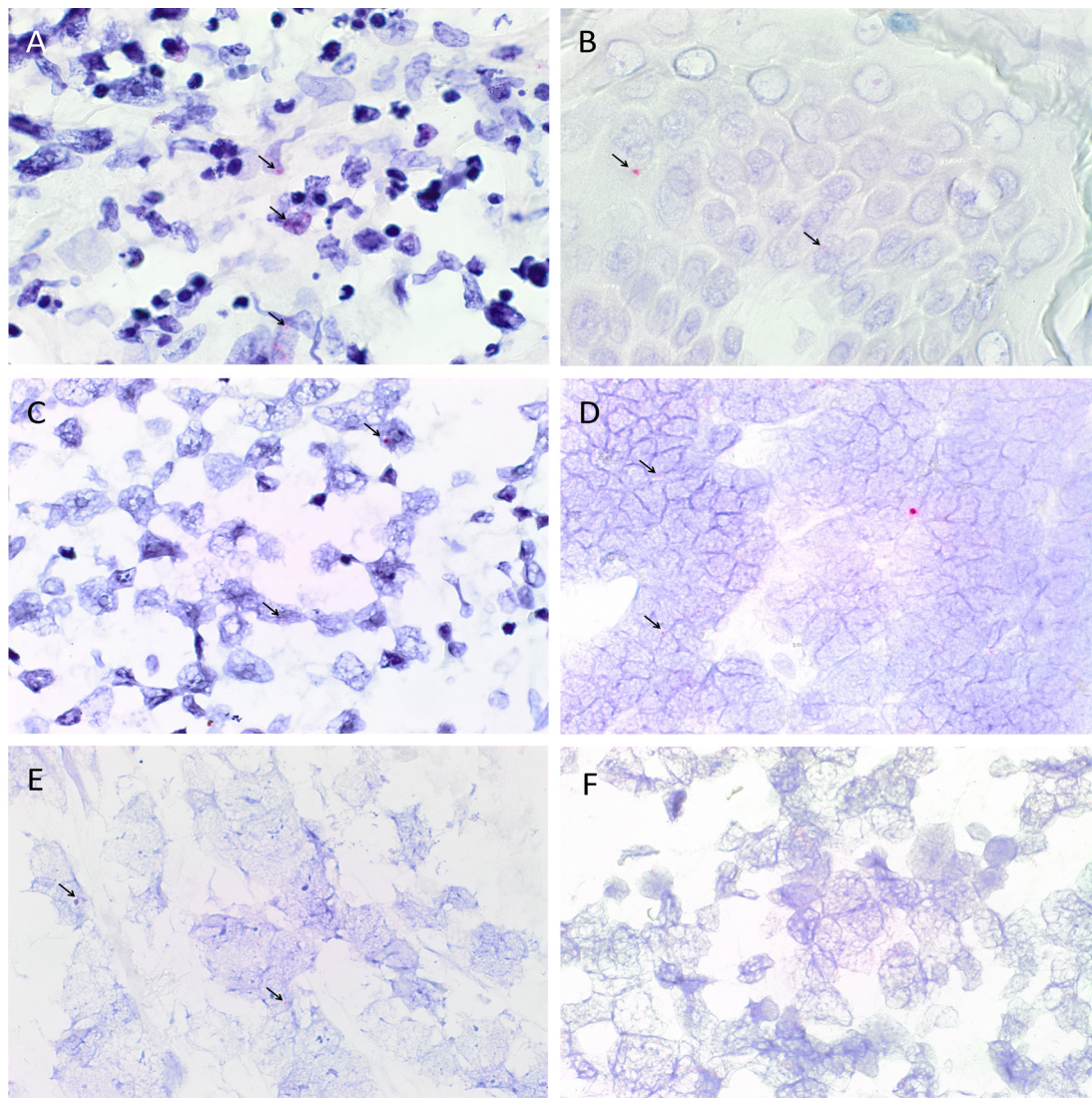


**Figure 8:** Positive human control *in situ* hybridization stained sections of seminoma for NANOG (A pink, *arrows*), skin for SOX2 (B pink, *arrows*), seminoma for OCT4 (C, pink, *arrows*), normal prostate tissue for c-MYC (D pink, *arrows*) and breast cancer (E, pink, *arrows*). Negative control (F) performed on a section of *Bacillus* confirmed the specificity of the secondary antibody. Nuclei were counter-stained with hematoxylin (A-F, blue). Original magnification: 1000x

## Discussion

There is a growing body of evidence supporting the crucial role of CSCs in cancer development and proliferation<sup>[14]</sup> with the expression of CSC markers being linked to poor prognosis<sup>[5,27]</sup>. In this study, DAB IHC staining showed the expression of the progenitor cell marker CD44 as reported in previous studies<sup>[23,24]</sup> and ESC markers NANOG, SOX2, OCT4, c-MYC and KLF4, in all ten RCCC samples examined. Expression of these five ESC markers was confirmed by ISH, which showed the presence of mRNA transcripts for all five ESC markers in all the ten RCCC samples studied. NanoString mRNA analysis demonstrated the expression of c-MYC and KLF4, NANOG and OCT4 relative to the housekeeping gene, GUSB. Interestingly the expression of SOX2 was below detectable levels in all four samples studied. This finding may be explained, in-part, by the degradation of RNA in the samples.

KLF4 has been associated with tumor suppressor functions in various cancer types including melanoma, breast cancer and RCC<sup>[21,35]</sup>. Our study demonstrated relatively low expression of KLF4 by IHC staining, but with higher levels of expression by NanoString mRNA analysis, which may be attributed to sampling bias.

Intiguently the high proportion of cells staining positively for SOX2 by DAB IHC staining was supported by ISH, but not

NanoString mRNA analysis. This transcriptional finding is consistent with other reports, which have shown decreased transcriptional expression of SOX2 in RCC compared to normal tissue<sup>[27]</sup>. The relatively high proportion of cells that stained positively on IHC staining may represent potentially ‘hang-over protein’ following transcriptional deactivation.

NANOG was expressed at high abundance by IHC staining and by NanoString mRNA analysis. This finding is in contrast to a recent report showing decreased expression of NANOG in RCC<sup>[27]</sup> although that study included all types of RCC, and not just RCCC.

We have observed a high abundance of c-MYC by IHC staining and NanoString analysis. IF IHC staining demonstrated co-expression of c-MYC with both the SOX2 and NANOG by immuno-reactive cells, with a subpopulation of the c-MYC<sup>+</sup> cells also expressing KLF4. This suggests that the more abundant CSCs express SOX2, NANOG and c-MYC, with a putative subset of these cells that also expresses KLF4, although this remains a topic of further investigation.

IHC staining showed a similar abundance of cells expressing OCT4, as that for KLF4. It is intriguing that that only some of the cells that express SOX2 and NANOG, while all of the cells that express KLF4 also express OCT4. We therefore infer that the OCT4<sup>+</sup> cells are a subset of NANOG<sup>+</sup>/SOX2<sup>+</sup> CSCs and propose that the OCT4<sup>+</sup>/KLF4<sup>+</sup> cells represent a relatively less abundant but putatively more primitive CSCs, consistent with a putative hierarchy in glioblastoma<sup>[18,36]</sup>.

Our study shows the expression of progenitor cell marker CD44 in RCCC using IHC staining, as reported in a large body of literature to identify CSCs in RCC<sup>[15]</sup> and we have expanded the panel of markers to include ESC markers NANOG, SOX2, OCT4, c-MYC, KLF4 which are markers also involved in iPSC<sup>[16,17]</sup>. IHC staining showed relatively high expression of CD44 co-expressed with SOX2 and NANOG. This suggests the presence of putative progenitor cells within RCCC that also express the ESC markers<sup>[15,24]</sup>.

Taken together it is exciting to speculate that the most abundant and potentially the most ‘mature’ CSC phenotype in RCCC is the SOX2<sup>+</sup>/NANOG<sup>+</sup>/c-MYC<sup>+</sup> subpopulation with a subset that also express KLF4 and OCT4, being the most ‘primitive’ CSC phenotype. However, the proof of this is beyond the scope of this study.

There is evidence supporting the presence of a hierarchy in CSCs<sup>[18,36]</sup>. Our findings suggest the putative presence of CSC heterogeneity within RCCC<sup>[37,38]</sup>, with a more primitive and least abundant CSCs expressing OCT4 and KLF4, and a more downstream CSC phenotype expressing SOX2, NANOG, and c-MYC, although further work is needed to conclusively determine this.

A limitation to the study is the relatively small sample size, however, our novel findings may shed light on a putative CSC hierarchy in RCCC, and future larger studies are required to confirm the significance of this.

Previous reports have shown an increased rate of metastases and a lower survival in patients with RCC that express ESC markers<sup>[5]</sup>, highlighting the need for further investigation into the use of ESC markers to monitor disease progression and treatment outcome. It is hoped that this research will add to the current knowledge of CSCs in RCC and provide a basis for further research into this very exciting field of research.

CSCs are present in RCCC and with a spectral abundance level at both the transcriptional and translational levels. These findings are in support of heterogeneity of CSC phenotypes within RCCC.

### Authors’ Contributions

- Conception and Design: TI and ST formulated the study hypothesis. TI, ST and AK-S designed the study.
- Administration and Support: ST and TI.
- Provision of study materials or patients: Gillies McIndoe Research Institute Tissue Bank and AK-S.
- Collection and assembly of data: RC, ST and TI.
- Data analysis and interpretation: RC, SS, TI, ST and HB interpreted the IHC and CISH data. TI, RC and ST interpreted the NanoString data. RM performed the statistical analysis.
- Manuscript writing: RC, ST, TI drafted the manuscript.
- Final approval of manuscript: All authors.

### Acknowledgements

The authors thank Ms Liz Jones and Ms Susana Enriquez of the Gillies McIndoe Research Institute for their assistance in IHC and ISH staining processed the tissues for NanoString analysis, respectively. RC was supported by a summer scholarships from the Deane Endowment Trust. Aspects of this work was presented, in part, at the 10<sup>th</sup> International Conference on cancer stem cells and Oncology Research, London, UK, June 26-27, 2017; and the Urological Society of Australia and New Zealand Conference, Tauranga, NZ, October 11-13, 2017.

### Funding

None

### Conflict of Interest

The authors declare that the research was conducted in the absence of any commercial or financial relationships that could be construed as a potential conflict of interest. TI and STT are inventors of the PCT patents Cancer Diagnosis and Therapy (PCT/NZ2015/050108), and Cancer Therapeutic (PCT/NZ2018/050006), and provisional patent application Novel Pharmaceutical Compositions for Cancer Therapy (US/62/711709).

## Ethics Approval

This study was approved by the Northern B Health and Disability Ethics Committee (Ref. 16/NTB/10).

## References

- Jonasch, E., Gao, J., Rathmell, W.K. Renal cell carcinoma. (2014) *BMJ* 349: 4797.  
[PubMed](#) | [Crossref](#) | [Others](#)
- Chow, W.H., Dong, L.M., Devesa, S.S. Epidemiology and risk factors for kidney cancer. (2010) *Nat Rev Urol* 7(5): 245-257.  
[PubMed](#) | [Crossref](#) | [Others](#)
- Huang, T.B., Ding, P.P., Chen, J.F., et al. Dietary fiber intake and risk of renal cell carcinoma: evidence from a meta-analysis. (2014) *Med Oncol* 31(8):125.  
[PubMed](#) | [Crossref](#) | [Others](#)
- Koul, H., Huh, J.S., Rove, K.O., et al. Molecular aspects of renal cell carcinoma: a review. (2011) *Am J Cancer Res* 1(2): 240-254.  
[PubMed](#) | [Crossref](#) | [Others](#)
- Cheng, B., Yang, G., Jiang, R., et al. Cancer stem cell markers predict a poor prognosis in renal cell carcinoma: a meta-analysis. (2016) *Oncotarget* 7(40): 65862-65875.  
[PubMed](#) | [Crossref](#) | [Others](#)
- Heng, D.Y., Kollmannsberger, C., Chi, K.N. Targeted therapy for metastatic renal cell carcinoma: current treatment and future directions. (2010) *Ther Adv Med Oncol* 2(1): 39-49  
[PubMed](#) | [Crossref](#) | [Others](#)
- Lee-Ying, R., Lester, R., Heng, D. Current management and future perspectives of metastatic renal cell carcinoma. (2014) *Int J Urol* 21(9): 847-855.  
[PubMed](#) | [Crossref](#) | [Others](#)
- Yuan, Z.X., Mo, J., Zhao, G., et al. Targeting strategies for renal cell carcinoma: from renal cancer cells to renal cancer stem cells. (2016) *Front Pharmacol* 7: 423.  
[PubMed](#) | [Crossref](#) | [Others](#)
- Motzer, R.J., Escudier, B., McDermott, D.F., et al. Nivolumab versus everolimus in advanced renal-cell carcinoma. (2015) *N Engl J Med* 373(19): 1803-1813.  
[PubMed](#) | [Crossref](#) | [Others](#)
- Motzer, R.J., Tannir, N.M., McDermott, D.F., et al. Nivolumab plus ipilimumab versus sunitinib in advanced renal-cell carcinoma. (2018) *N Engl J Med*. 378(14): 1277-1290.  
[PubMed](#) | [Crossref](#) | [Others](#)
- Linehan, W.M., Grubb, R.L., Coleman, J.A., et al. The genetic basis of cancer of kidney cancer: implications for gene-specific clinical management. (2005) *BJU Int* 95(2): 2-7.  
[PubMed](#) | [Crossref](#) | [Others](#)
- Myszczyzyn, A., Czarnecka, A.M., Matak, D., et al. The role of hypoxia and cancer stem cells in renal cell carcinoma pathogenesis. (2015) *Stem Cell Rev* 11(6): 919-943.  
[PubMed](#) | [Crossref](#) | [Others](#)
- Zhao, W., Ji, X., Zhang, F., et al. Embryonic stems cell markers. (2012) *Molecules* 17(6): 6196-6236.  
[PubMed](#) | [Crossref](#) | [Others](#)
- Schoenhals, M., Kassambara, A., De Vos, J., et al. Embryonic stem cell markers expression in cancers. (2009) *Biochem Biophys Res Commun* 383(2): 157-162.  
[PubMed](#) | [Crossref](#) | [Others](#)
- Peired, A.J., Sisti, A., Romagnani, P. Renal cancer stem cells: Characterization and targeted therapies. (2016) *Stem Cells Int* 2016: 8342625.  
[PubMed](#) | [Crossref](#) | [Others](#)
- Takahashi, K., Yamanaka, S. Induction of pluripotent stem cells from mouse embryonic and adult fibroblast cultures by defined factors. (2006) *Cell* 126(4): 663-676.  
[PubMed](#) | [Crossref](#) | [Others](#)
- Yu, J., Thomson, J.A. Pluripotent stem cell lines. (2008) *Genes Dev* 22(15): 1987-1997.  
[PubMed](#) | [Crossref](#) | [Others](#)
- Bradshaw, A., Wickremsekera, A., Tan, S.T., et al. Cancer stem cell hierarchy in glioblastoma multiforme. (2016) *Front Surg* 3: 21.  
[PubMed](#) | [Crossref](#) | [Others](#)
- Yu, F., Li, J., Chen, H., et al. Kruppel-like factor 4 (KLF4) is required for maintenance of breast cancer stem cells and for cell migration and invasion. (2011) *Oncogene* 30(18): 2161-2172.  
[PubMed](#) | [Crossref](#) | [Others](#)
- Song, E., Ma, X., Li, H., et al. Attenuation of kruppel-like factor 4 facilitates carcinogenesis by inducing g1/s phase arrest in clear cell renal cell carcinoma. (2013) *PLoS One* 8(7): 67758.  
[PubMed](#) | [Crossref](#) | [Others](#)
- Li, H., Wang, J., Xiao, W., et al. Epigenetic alterations of Kruppel-like factor 4 and its tumor suppressor function in renal cell carcinoma. (2013) *Carcinogenesis* 34(10): 2262-2270.  
[PubMed](#) | [Crossref](#) | [Others](#)
- Tang, S.W., Chang, W.H., Su, Y.C., et al. MYC pathway is activated in clear cell renal cell carcinoma and essential for proliferation of clear cell renal cell carcinoma cells. (2009) *Cancer Lett* 273(1): 35-43.  
[PubMed](#) | [Crossref](#) | [Others](#)
- Corrò, C., Moch, H. Biomarker discovery for renal cancer stem cells. (2018) *J Pathol Clin Res* 4(1): 3-18.  
[PubMed](#) | [Crossref](#) | [Others](#)
- Sagrinati, C., Netti, G.S., Mazzinghi, B., et al. Isolation and characterization of multipotent progenitor cells from the Bowman's capsule of adult human kidneys. (2006) *J Am Soc Nephrol* 17(9): 2443-2456.  
[PubMed](#) | [Crossref](#) | [Others](#)
- Terpe, H.J., Störkel, S., Zimmer, U., et al. Expression of CD44 isoforms in renal cell tumors. Positive correlation to tumor differentiation. (1996) *Am J Pathol* 148(2): 453-463.  
[PubMed](#) | [Crossref](#) | [Others](#)
- Li, N., Tsuji, M., Kanda, K., et al. Analysis of CD44 isoform v10 expression and its prognostic value in renal cell carcinoma. (2008) *BJU International* 85 (4): 514-518.  
[PubMed](#) | [Crossref](#) | [Others](#)
- Liu, Y., Zhang, C., Fan, J., et al. Comprehensive analysis of clinical significance of stem-cell related factors in renal cell cancer. (2011) *World J Surg Oncol* 9: 121.  
[PubMed](#) | [Crossref](#) | [Others](#)

28. Tan, E.M., Chudakova, D.A., Davis, P.F., et al. Characterisation of subpopulations of myeloid cells in infantile haemangioma. (2015) *J Clin Pathol* 68(7): 571-574.  
[Pubmed](#) | [Crossref](#) | [Others](#)
29. Ezech, U.I., Turek, P.J., Reijo, R.A., et al. Human embryonic stem cell genes OCT4, NANOG, STELLAR, and GDF3 are expressed in both seminoma and breast carcinoma. (2005) *Cancer* 104(10): 2255-2265.  
[Pubmed](#) | [Crossref](#) | [Others](#)
30. Laga, A.C., Lai, C.Y., Zhan, Q., et al. Expression of the embryonic stem cell transcription factor SOX2 in human skin: relevance to melanocyte and merkel cell biology. (2010) *Am J Pathol* 176(2): 903-913.  
[Pubmed](#) | [Crossref](#) | [Others](#)
31. Fan, L., Peng, G., Sahgal, N., et al. Regulation of c-Myc expression by the histone demethylase JMJD1A is essential for prostate cancer cell growth and survival. (2016) *Oncogene* 35(19): 2441-2452.  
[Pubmed](#) | [Crossref](#) | [Others](#)
32. Prince, M.E., Sivanandan, R., Kaczorowski, A., et al. Identification of a subpopulation of cells with cancer stem cell properties in head and neck squamous cell carcinoma. (2007) *Proc Nat Acad Sci USA* 104(3): 973-978.  
[Pubmed](#) | [Crossref](#) | [Others](#)
33. Itinteang, T., Marsh, R., Davis, P.F., et al. Angiotensin II causes cellular proliferation in infantile haemangioma via angiotensin II receptor 2 activation. (2015) *J Clin Pathol* 68(5): 346-350.  
[Pubmed](#) | [Crossref](#) | [Others](#)
34. Yu, H.H., Featherston, T., Tan, S.T., et al. Characterization of cancer stem cells in moderately differentiated buccal mucosal squamous cell carcinoma. (2016) *Front Surg* 3: 46.  
[Pubmed](#) | [Crossref](#) | [Others](#)
35. Rivero, M., Montagnani, V., Stecca, B. KLF4 is regulated by RAS/RAF/MEK/ERK signaling through E2F1 and promotes melanoma cell growth. (2017) *Oncogene* 36(23): 3322-3333.  
[Pubmed](#) | [Crossref](#) | [Others](#)
36. Koh, S.P., Wickremesekera, A.C., Tan, S.T., et al. Editorial: fate mapping of human glioblastoma reveals an invariant stem cell hierarchy. (2018) *Transl Cancer Res* 7(4).  
[Pubmed](#) | [Crossref](#) | [Others](#)
37. Tang, D.G. Understanding cancer stem cell heterogeneity and plasticity. (2012) *Cell Res* 22(3): 457-472  
[Pubmed](#) | [Crossref](#) | [Others](#)
38. Rich, J.N. Cancer stem cells: understanding tumor hierarchy and heterogeneity. (2016) *Medicine* 95(1): 2-7.  
[Pubmed](#) | [Crossref](#) | [Others](#)

Submit your manuscript to Ommega Publishers and we will help you at every step:

- We accept pre-submission inquiries
- Our selector tool helps you to find the most relevant journal
- We provide round the clock customer support
- Convenient online submission
- Thorough peer review
- Inclusion in all major indexing services
- Maximum visibility for your research

Submit your manuscript at



<https://www.ommegaonline.org/submit-manuscript>